Z. Physik A 286, 173–180 (1978)

Zeitschrift
für Physik A

The ^{8}Be Scattering System in the Framework of a Microscopic Theory*

H. Stöwe and W. Zahn**
Institut für Theoretische Physik der Universität zu Köln, Köln, Germany

Received October 4, Revised Version December 22, 1977

We present conclusions for the ^{8}Be scattering system from a multi-channel calculation in the framework of a microscopic nuclear cluster model. The energy region from α-α threshold up to 30 MeV center of mass is investigated; results of an eigenphase analysis for J^π-values from 0^+ to 4^+ and 0^- to 4^- are displayed. For comparison and completion we have performed quasibound state calculations taking into account possible combinations of participating structures. The results throw light upon a complicated sequence of resonant states and moreover predict the occurrence of some additional levels in the energy spectrum.

1. Introduction

In recent years increasing interest has been taken in the eight-nucleon problem and especially in the ^{8}Be scattering system. In the energy region from α-α threshold up to about 30 MeV c.m. experimental investigations have disclosed more or less complicated sequences of scattering states [1–12]. In this context the most interesting energy region seems to be between the ^{7}Li-p threshold (17.256 MeV) and about 25 MeV where several thresholds with fragments stable under particle decay are found.

Theoretical investigations of the ^{8}Be scattering system have used the usual approaches. There are the intermediate coupling version of the shell model which was applied to (1 p)-shell nuclei for mass numbers $4 < A \leqq 16$ [13, 14] and shell model calculations for (1 p)-shell nuclei using simple effective interactions [15, 16]. Approaches using many-level R-matrix theory [17], projected Hartree-Fock calculations [18], and configuration interaction calculations [19, 20, 21] which allow for collective motion, were reported. However, all these calculations could not bring the diverse experimental findings into one coherent description. To amend this situation deformed ^{8}Be nuclei were proposed in [16]. Investigations in the framework of the cluster model picture can take that demand into account.

Recently, attempts have been undertaken to perform microscopic multi-channel cluster model calculations for the eight-nucleon problem [22–25]. A two-channel α-α, α-α^* calculation [22] yielded first results of greater importance. It could be shown that the ground state rotational band of the α-α configuration is duplicated above the α-α^* threshold with a moment of inertia about a factor of two larger than that of the ground-state band. In the meantime there is strong experimental evidence that this band actually appears [25]. A multi-channel cluster model calculation for the reactions ^{7}Li$(p,p)^7$Li and ^{7}Li$(p,n)^7$Be [23] gave a first microscopic description of the ^{8}Be scattering system in the energy region from the ^{7}Li-p threshold at 17.256 MeV up to about 19.5 MeV c.m.

That calculation, however, was still afflicted with some characteristic insufficiencies of former calculations. In the meantime the difficulties could be overcome and an impressively good description of the ^{8}Li scattering system could be given (cf. [24]), disclosing correlations of a complicated reaction

* Work supported by the "Bundesministerium für Forschung und Technologie"

** Present address: Department of Physics, The University of Michigan, Ann Arbor, MI 48109, USA

0340-2193/78/0286/0173/$01.60

mechanism. In addition the complementary significance of scattering- and bound- and quasibound state calculations for the eight-nucleon problem could be shown.

Starting with the experiences made so far we have performed microscopic cluster model calculations for the ^{8}Be scattering system. The scattering calculation is essentially an extension of the calculation reported in [23]: We use a modified effective spin-orbit force, include additional channels for $J^\pi = 3^+$, and calculate the S-matrix over a larger energy range. In Section 2 we shall briefly outline the relevant details of our calculations. In Section 3 we present calculated eigenphases and – where necessary for elucidation – call to notice diagonal phase shifts and channel coupling strengths. In Section 4 results of quasibound state calculations are displayed and interpreted. Finally, in Section 5 we shall give a comprehensive discussion of the results found in the unterlying calculations and compare them with results obtained from recent ^{8}Li calculations [24].

2. The Calculation

Our method has been described in great detail elsewhere (cf., e.g., [24, 26]) and so we may focus our considerations on the essential points.

We use the Kohn-Hulthén variational procedure with multi-channel testfunctions of the refined cluster type and a force derived from two-nucleon data. The spin-orbit force is multiplied by a factor of (A/2-1) according to recent findings [24, 28].

For the present calculation we shall take into account all systems which consist of two fragments stable under particle decay. These are the fragmentations α-α, ^{7}Li-p, ^{7}Li*-p, ^{7}Be-n, ^{7}Be*-n, and ^{6}Li-d. The corresponding wave functions and parameters are given in the Appendix. Angular momenta $L = 0, 2, 4$ in the relative motion of the α-α fragments, and $L = 0, 1, 2$ for ^{7}Li-p, ^{7}Li*-p, ^{7}Be-n, ^{7}Be*-n, are considered. For $J^\pi = 3^+$ the additonal allowance for $L = 3$ is necessary since otherwise the ^{7}Li*-p and ^{7}Be*-n structures would be excluded from our consideration for that case. We shall see later that just these fragmentations are responsible for some interesting features. In the relative motion of ^{6}Li-d angular momenta $L = 0, 1, 2, 3$ are taken into account. As a result we end up with the following numbers n of coupled channels per J^π-value

J^π	0^+	1^+	2^+	3^+	4^+	0^-	1^-	2^-	3^-	4^-
n	7	11	11	12	2	5	14	14	10	4

if all channels are allowed for simultaneously. In Table 1 we have compared experimental and calculated threshold energies relative to the ^{7}Li-p threshold for the fragmentations which are stable under particle decay.

Table 1. Experimental and calculated threshold energies in MeV relative to the ^{7}Li-p threshold

	Experimental (Ref. 1)	Calculated
^{6}Li-d	5.026	3.886
^{7}Be*-n	2.073	1.983
^{7}Be-n	1.644	1.272
^{7}Li*-p	0.478	0.724
^{7}Li-p	0.	0.
α-α	−17.348	−16.584

Some features of the S-matrix can be understood by examining the eigenphases; these are the numbers δ_l defined via

$$S_{ij} = \sum_l U_{il} \exp\{2i\delta_l\} U^*_{lj}.$$

Here S denotes the total S-matrix and U an orthogonal transformation. The quasibound state calculations are performed using the relative parameter set indicated by 7–11 in [24].

A ^{8}Be calculation that in addition to the above quoted structures, allows for the ^{5}He – ^{3}He and ^{5}Li-t structures cannot be performed because of technical reasons due to restricted computer capacities. In principle, one could replace in a further calculation e.g. the ^{6}Li-d structure by the ^{5}He – ^{3}He and ^{5}Li-t structures and by this solve the storage problem. However, the present calculation took about 22 hours of computational time at the CDC 7600 of the computing center at the University of Cologne. As a consequence a further calculation of at least the same extent cannot be justified in this context.

In a recent ^{8}Li calculation [24] the influence of the ^{5}He-t structure has been studied intensely. The ^{5}He – ^{3}He and ^{5}Li-t structures should act analogously on the coupled-channel calculation for the ^{8}Be scattering system. So, with the aid of the various data presented in the ^{8}Li calculation reasonable conclusions from analogy may be deduced for the ^{8}Be scattering system.

The influence of the α-α^* channel in the energy region around the α-α^* threshold at 20.2 MeV has been discussed in a separate paper [27]. This could be done since the coupling of the α-α^* channel to all other channels is less than 4% [28].

3. Results of the Scattering Calculation

In this Section we shall discuss results of a scattering calculation and partition the energy region into three fields of different relevance:

3.1. $0\,MeV \leqq E_x \leqq 16\,MeV$

From α-α threshold up to about 16 MeV center of mass the scattering states are very simple and may be interpreted by a simple model of two rotating α clusters. The corresponding findings of [29] are reproduced, however, for $J^\pi = 2^+$ the resonance energy is lowered from 3 MeV to 1.5 MeV. This is due to the allowance for the additional distortion channels.

3.2. $16\,MeV \leqq E_x \leqq 23\,MeV$

From ^{7}Li-p threshold up to about 23 MeV c.m. a complicated sequence of scattering states has been revealed by experimental investigations, that sequence being due to a relatively large number of different fragmentations that begin to provide a considerable influence in a comparatively narrow energy region. For the energy region from the ^{7}Li-p threshold up to 19.5 MeV c.m. the diagonal phase shifts reported in [23] do not change qualitatively in the present calculation; so we can refer to these curves without plotting them again. In [23] the experimental and calculated cross sections for the reactions ^{7}Li$(p,p)^7$Li and ^{7}Li$(p,n)^7$Be are compared by shifting the energies according to the different thresholds. As this method is not suited very well for the inspection of details we do not report the new results for the cross sections. In Figure 1 we display eigenphases for J^π-values where resonant behavior occurs, having regard to the no-crossing rule for different eigenphases that belong to one J^π-value. The eigenphases are plotted versus c.m. energies relative to the calculated ^{7}Li-p threshold. In the following we shall discuss all resonant states separately. According to a usual procedure [30] we take the resonance energies as the turning points of the curvature of the phases.

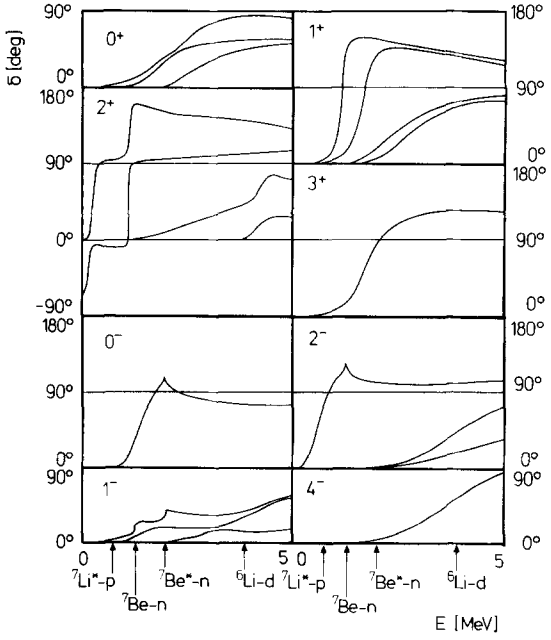

Fig. 1. Eigenphases for J^π-values where resonant behavior occurs versus excitation energy

3.2.1. Positive Parity States

$J^\pi = 0^+$: Three resonant states at 1.8, 2.1, and 2.8 MeV can be read off from the eigenphases. At present, corresponding levels have not yet been disclosed by experimental investigations.

$J^\pi = 1^+$: Four resonant states appear at 1.1, 1.6, 2.4, and 2.8 MeV. The lower two of them may be related to the experimentally detected states at 17.64 and 18.15 MeV.

$J^\pi = 2^+$: Two levels below the ^{7}Li-p threshold are found experimentally. In the present calculation, however, two narrow resonant states appear above the ^{7}Li-p threshold at 0.35 MeV and 1.15 MeV. This defect is due to the neglect of the ^{5}He$-^3$He and ^{5}Li-t structures and is well-known from the ^{8}Li calculation: With the ^{5}He-t channel the binding energy of the corresponding 2^+ state is lowered by 1.1 MeV. At about 3.3 MeV a broad resonance is found, the S-matrix yielding an inelastic parameter close to one. On the first glance it would be tempting to identify this state with the experimentally detected 2^+ state at 20.1 MeV. However, experiment has yielded a comparatively narrow width of about 1.1 MeV for that state and a strong inelasticity of $\eta \sim 0.3$ (cf. [2, 27]). Directly above the ^{6}Li-d threshold a resonant state with $J^\pi = 2^+$ appears that is strongly coupled to the other channels. In a general treatise about narrow resonances at thresholds in light nuclei Hackenbroich and Seligman [31] have classified this state as a threshold state. Their prediction has claimed parallel intrinsic angular momenta and reaction partners in relative S-states. In fact, our calculation supports the considerations of [31] by producing a sharp resonant behavior of the phase shift in the ^{6}Li-d channel with quantum numbers $L=0$, $S=2$, directly above the ^{6}Li-d threshold.

$J^\pi = 3^+$: One resonant state is found at 1.7 MeV. The appearance of this state is due to the important influence of the (still closed) ^{6}Li-d channel yielding a strong coupling of the ^{7}Li-p and ^{7}Be-n structures (cf., e.g., [23], Fig. 4). Omission of the ^{6}Li-d channel leads to a very small coupling of ^{7}Li-p and ^{7}Be-n channels. Note, however, that even above ^{6}Li-d threshold the ^{6}Li-d channel is only weakly coupled to the other channels. That is to say, if one allows for the ^{6}Li-d configuration the scattering process may proceed via

an intermediate ^{6}Li-d stage and both proton or neutron decay are possible. This two-step behavior is in agreement with experimental experiences. A second 3^+ resonant state is not found due to the neglect of the ^{5}He$-^3$He and ^{5}Li-t structures. This may be concluded by way of analogy from [24].

$J^\pi = 4^+$: No resonant behavior is found. From this we can conclude that the experimentally detected 4^+ state at 19.9 MeV is not generated by the employed fragmentations and relative angular momenta, and other structures must be responsible for the occurrence of that state (cf. [27]).

3.2.2. Negative Parity States

$J^\pi = 0^-$: One resonant state at 1.35 MeV and a Wigner cusp at the ^{7}Be*-n threshold appear. Corresponding states have not yet been disclosed by experiment.

$J^\pi = 1^-$: The eigenphase shift exhibits a Wigner cusp at the ^{7}Be-n threshold and another Wigner cusp at the ^{7}Be*-n threshold. This second cusp may be related to the experimentally found 1^- state at 19.4 MeV.

$J^\pi = 2^-$: A threshold state positioned directly below the ^{7}Li*-p threshold appears and the same argumentation as for the 2^+ resonance at the ^{6}Li-d threshold applies. It is tempting to identify this threshold state with the experimentally detected 2^- state at 18.91 MeV. Above that, the 2^- phase shift bends into a Wigner cusp at the ^{7}Be-n threshold.

$J^\pi = 3^-$: Nothing remarkable is found besides of two extremely broad structures localized anywhere between 4 and 7.5 MeV. One such resonance has already been found in a ^{8}Li calculation [24].

$J^\pi = 4^-$: A broad resonant behavior occurs at about 3.5 MeV. This state may be related to the experimentally found 4^- state at 20.9 MeV. Furthermore a second extremely broad 4^- structure with about the same position and localization as the 3^- states appears.

3.3. 23 MeV $\leqq E_x \leqq$ 30 MeV

For higher energies, i.e. beyond 23 MeV, the calculated results turn out to be the following: The 2^+ eigenphase shift exhibits a resonant behavior about 3.5 MeV above the calculated ^{6}Li-d threshold. This state should obviously be related to the experimentally detected 2^+ state at 25.2 MeV. The corresponding phase shift curve is not plotted since it is the only one that exhibits a comparatively localized resonant behavior. In general, for energies beyond 23 MeV no more interesting features in the eigenphase shifts besides of two extremely broad 1^- and 2^- states, respectively, about 4 MeV above the calculated ^{6}Li-d threshold appear in our results. This is in reasonable agreement with experiment [1] since on one hand only extremely broad 1^-, 2^- structures at about 24 MeV with widths of 8 MeV have been found. On the other hand, the occurrence of the experimentally detected levels in the energy region up to 30 MeV c.m. (except of the $J^\pi = 0^+$, $T = 2$, analog of the ^{8}He ground state which cannot appear in our calculation) seems to be questionable (cf. [1]).

4. Results of Quasibound State Calculations

In this Section we present results of a series of quasibound state calculations. As discussed in [24], such calculations are a considerable succor if they are performed together with scattering calculations. Significant information can be obtained by omitting successively the channel with the highest-lying threshold in a series of quasibound state calculations. Mutual comparison of the corresponding results discloses the relevant structures that contribute to the physical states.

The results are displayed in Figure 2 and will be discussed in the following. The level scheme resulting from the scattering calculation discussed in the preceding Section is given in Figure 2a. The other columns of Figure 2 show spectra of quasibound state calculations allowing for different combinations of participating structures. We start with a calculation where all structures are included (Fig. 2b) and successively omit the structure with the highest threshold energy. In all these calculations the same set of radial parameters for the test functions is used that has proved to yield a reasonable reproduction of the resonance energies [24]. Of course, the spectra had to be truncated at a certain energy in order to avoid meaningless levels. Direct comparison of the calculated and the experimental spectrum seems not to be very significant since the positions of the calculated thresholds are rather inadequate (cf. Table 1).

For α-α, $J^\pi = 0^+$, a poor approximation to the experimental situation is found; the calculated ground state is weakly bound. There are two possible explanations: First, the description of the α-α fragmentation is of inferior quality, the α cluster being bound by 21.5 MeV instead of about 28.2 MeV. The corresponding α-α threshold results too high. Or second, we run into numerical difficulties concerning the radial dependence of our test functions. A comprehensive explanation would go beyond the limits of this work, but we would like to mention that our test

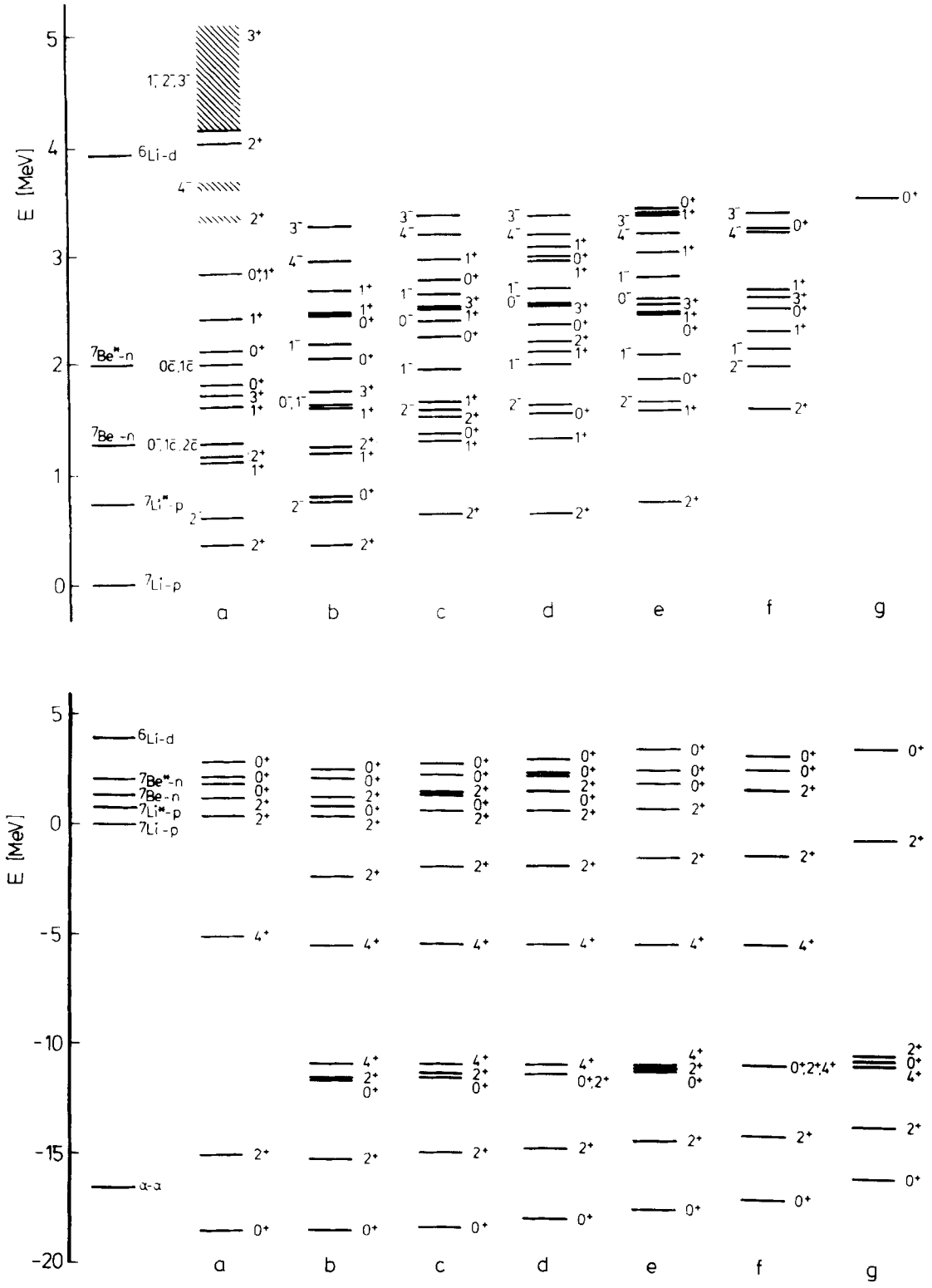

Fig. 2a–g. Level schemes of ^{8}Be. **a** from a scattering calculation, levels indicated by "c" are Wigner cusps, **b** from a quasibound state calculation with relative parameters 7–11 (cf. [24]), including all structures, **c** as **b** but without ^{6}Li-*d* structure, **d** as **c** but without ^{7}Be*-*n* structure, **e** as **d** but without ^{7}Be-*n* structure, **f** as **e** but without ^{7}Li*-*p* structure, **g** as **f** but without ^{7}Li-*p* structure. In the upper part all levels above ^{7}Li-*p* threshold are plotted. In the lower part the levels from a calculation including the α-α structure are plotted

functions start with R^0 whereas due to the Pauli principle better numerical stability is gained with test functions starting with R^4.

Our calculations show 0^+, 2^+, 4^+ states between the 2^+ and 4^+ states of the α-α rotational band. However, our corresponding scattering calculation does not give any evidence for the occurrence of such states and it therefore seems that these states are spurious. Suffice it to say, that quasibound state calculations, although being more sensitive than scattering calculations, should in critical cases only be interpreted with regard to experiences made in scattering calculations.

If one looks at Figure 2a and b one can say that in general good agreement for all J^π-values with the results of the scattering calculation is found. One exception is the 0^+ case and the above quoted explanations may be appertaining to that defect. From a comparison of Figure 2d and e one can learn that neglect of the ^{7}Be-n structure brings about the 2^+ and 1^+ states above ^{7}Li-p threshold once. If the ^{7}Be-n structure is allowed for, those structures appear twice.

Summarizing the experiences made here one must perceive that quasibound state calculations gave different information about the scattering system in recent ^{8}Li calculations [24] and in the present ^{8}Be calculations. In the ^{8}Be results appreciable changes are caused by the successive omission of the participating structures. Whereas the position of the second calculated 2^+ state above ^{7}Li-p threshold is drastically changed, the position of the first one is only slightly changed if the ^{7}Be-n and ^{7}Be*-n structures are omitted. Hence the appearance of the second state must be related to the structures ^{7}Li-p, ^{7}Li*-p and ^{7}Be-n, ^{7}Be*-n, respectively, and must be based upon a strong isospin mixture.

5. Discussion and Comparison of Different Microscopic Calculations

In the present work results of a microscopic multichannel calculation for the ^{8}Be scattering system and results of corresponding quasibound state calculations for comparison and completion have been presented. In this discussion we shall not only recapitulate the results of the present calculations but moreover broach the results achieved in recent ^{8}Li calculations [24]. This is in order to appreciate comprehensively the mutual and complementary capability of different calculations in the microscopic approach to give an elucidation of the eight-nucleon problem.

In the ^{8}Be system the ^{8}Li spectrum should be duplicated because of the existence of two isospin states and shifted towards higher energies because of the Coulomb repulsion. We want to stress once more one of the more outstanding findings of the ^{8}Li calculation, i.e. the influence of the ^{5}He-t structure on the scattering results. The same holds good by conclusion from analogy for the ^{5}He$-^3$He and ^{5}Li-t structures in ^{8}Be. If those structures are included, in general lowering of the resonance energies results; for $L=0$ states occurring at thresholds phases exhibit more distinctly pronounced resonant behavior, and at least one additional 3^+ resonance is expected. Further changes are expected that are caused by the additional α-α and ^{6}Li-d channels. However, for most of the J^π-values where results have been reported for, the practical situation looks somewhat differently:

5.1. Positive Parity States

$J^\pi=0^+$: Three resonant states appear and it is conceivable that one of them is caused either by the α-α channel or by a two-step process via the ^{6}Li-d intermediate structure.

$J^\pi=1^+$: Four resonant states are found compared to two resonant states which appear in ^{8}Li.

$J^\pi=2^+$: One bound state from ^{8}Li is faced by three scattering states in ^{8}Be. The lower two of them are the corresponding bound states which, however, come to lie above the ^{7}Li-p threshold since the ^{5}He $-^3$He and ^{5}Li-t structures are omitted (cf. [24]). The third one is the threshold state at the ^{6}Li-d threshold.

$J^\pi=3^+$: Two resonant states are expected to come from the ^{5}He$-^3$He and ^{5}Li-t structures and thus, of course, cannot appear in the present calculation. Only one state from a two-step process via a ^{6}Li-d intermediate stage is found.

$J^\pi=4^+$: Resonant states occur neither in ^{8}Li nor in ^{8}Be eigenphases.

5.2. Negative Parity States

$J^\pi=0^-$: The ^{8}Li calculation did not exhibit resonant behavior; for ^{8}Be one resonance is found in the ^{7}Li*-p, $L=0$, channel that is produced by the influence of the ^{7}Be*-n channel.

$J^\pi=1^-$: Here the situation is even more involved. The ^{8}Li calculation has yielded a resonant state at the ^{7}Li*-n threshold. A corresponding state in ^{8}Be is not found. This might be due to the Coulomb repulsion and missing ^{5}He$-^3$He and ^{5}Li-t structures. Instead of that expected resonance Wigner cusps in the ^{7}Li-p, $L=0$, and ^{7}Li*-p, $L=0$, channels appear

which are generated by the corresponding ^{7}Be-n, $L=0$, and ^{7}Be*-n, $L=0$, channels, respectively. Furthermore one would expect that the ^{7}Be*-n state can be observed in ^{7}Be-n. Nothing of the kind is found which might be related to the missing ^{5}He$-^3$He and ^{5}Li-t structures.

$J^\pi=2^-$: A resonant behavior in the form of a vertical rise of the eigenphase shift at the ^{7}Li-n threshold has been found in ^{8}Li. In the ^{8}Be results the corresponding eigenphase does not start vertically because of the Coulomb repulsion. Instead of this we find a clear-cut resonant behavior in the ^{7}Li-p, $L=0$, phase which bends into a Wigner cusp at the ^{7}Be-n threshold. In the corresponding ^{7}Be-n, $L=0$, channel such a behavior is not observed and the same argument as in the 1^- case applies. However, one question remains open: Why does this resonant behavior starting at threshold, occur in the 2^- eigenphase shift only but not in the 1^- eigenphase shift in ^{8}Be?

$J^\pi=3^-$: In agreement with expectation two extremely broad rises of phase shifts at higher energies are found.

$J^\pi=4^-$: A similar behavior as for the 3^- case occurs, however, the lower one of the states being somewhat more pronounced in the eigenphase shift. In agreement with the ^{8}Li results the 4^- states are located a little lower than the 3^- states.

Finally, the present calculation has provided us in addition with extremely broad 1^- and 2^- structures beyond 23 MeV.

5.3. Final Remarks

This work together with recent publications concerning the eight-nucleon problem [23, 24, 28] proves the microscopic approach to be a powerful tool for the investigation and elucidation of nuclear systems with higher mass numbers. For all that, we want to emphasize once more in conclusion that one point should not be passed over in silence. The results of the present work demonstrate distinctly where limits of our microscopic approach exist. In this work we have covered a large energy region. This implies large interaction regions in our calculations and thus an increasing number of nodes in the wave functions per unit volume. The employed method requires the approximation of the wave functions by square-integrable functions and thus becomes numerically more and more problematic the larger the energy region is. We want to emphasize especially, that it is not the increasing number of particles that arises problems but the considerable extent of the energy range that has to be covered in a ^{8}Be calculation. Therefore, investigations in even more complex systems with high-lying thresholds cannot be vindicated before computational techniques have been developed that go far beyond the present stage of application.

Appendix

The explicit form of the wave function for fragments with up to four particles $2\leqq n\leqq 4$ is given by

$$\varphi(\mathbf{r}_1,\ldots,\mathbf{r}_n)=\sum_{m=1}^{M} c_m \cdot \exp\left\{-\frac{1}{n}\beta_m \sum_{1\leqq i<k\leqq n}(\mathbf{r}_i-\mathbf{r}_k)^2\right\}\Xi^j \tag{A.1}$$

and for fragments with more than four particles by

$$\varphi(\mathbf{r}_1,\ldots,\mathbf{r}_n)=\sum_{m=1}^{M} c_m \cdot \exp\left\{-\frac{1}{n_1}\beta_m \sum_{1\leqq i<k\leqq n_1}(\mathbf{r}_i-\mathbf{r}_k)^2 -\frac{1}{n_2}\gamma_m \sum_{n_1<i<k\leqq n}(\mathbf{r}_i-\mathbf{r}_k)^2-\delta_m\mathbf{R}^2\right\} R^l[Y_l(\Omega_{\mathbf{R}})\,\Xi^s]^j. \tag{A.2}$$

Table 2. Parameters used in (A.1) and (A.2). Here E_B is given in MeV; the parameters c_m, β_m, γ_m, δ_m are given in fm^{-2}

Fragment	$\lvert E_B\rvert$	j	l	n	n_1	M	c_m	β_m	γ_m	δ_m
^{2}H	1.352	1/2		2		2	0.5320	0.3204		
							0.1492	0.0403		
^{4}He	21.476	0		4		2	5.2018	0.3240		
							0.0658	0.0840		
^{6}Li	21.086	1	0	6	4	1	1.0000	0.2768	0.2369	0.0420
^{7}Li	26.240	3/2	1	7	4	2	8.2287	0.3169	0.2895	0.0434
^{7}Li*	25.757	1/2					0.4519	0.2207	0.1201	0.0298
^{7}Be	25.020	3/2	1	7	4	3	0.3898	0.2439	0.1070	0.0259
^{7}Be*	24.546	1/2					1.2116	0.3076	0.3234	0.0142
							6.9461	0.2910	0.2473	0.0708

Here $n=n_1+n_2$ is the partition into two clusters, Ξ denotes appropriate spin-isospin functions, and R is the normalized relative vector between the clusters

$$\mathbf{R}=\sqrt{\frac{n_2}{n_1 n}}\sum_{i=1}^{n_1}\mathbf{r}_i-\sqrt{\frac{n_1}{n_2 n}}\sum_{i=n_1+1}^{n}\mathbf{r}_i. \tag{A.3}$$

The parameters used in (A.1) and (A.2) for the description of the considered fragments are listed in Table 2.

Finally, the square integrable functions of the relative motion have the form

$$\chi_{k,m}(R_k)=\exp\{-\varepsilon_m R_k^2\}. \tag{A.4}$$

Where R_k is normalized according to (A.3). The parameters ε_m are taken as

5, 2.5, 1.7, 1.3, 0.9, 0.55, 0.35, 0.2, 0.1, 0.05, 0.025, 0.0125, 0.007, 0.004, 0.0015

and used as an independent set for all channels k [24].

References

1. Ajzenberg-Selove, F., Lauritsen, T.: Nucl. Phys. A **227**, 1 (1974)
2. Bacher, A.D., Resmini, F.G., Conzett, H.E., de Swiniarski, R., Meiner, H., Ernst, J.: Phys. Rev. Lett. **29**, 1331 (1972)
3. Brown, L., Steiner, E., Arnold, L.G., Seyler, R.G.: Nucl. Phys. A **206**, 353 (1973)
4. Rohrer, U., Brown, L.: Nucl. Phys. A **217**, 525 (1973)
5. Arnold, L.G., Seyler, R.G., Brown, L., Bonner, T.I., Steiner, E.: Phys. Rev. Lett. **32**, 895 (1974)
6. Burke, C.A., Lunnon, M.T., Lefevre, H.W.: Phys. Rev. C **10**, 1299 (1974)
7. King, C.H., Rossner, H.H., Austin, S.M., Chien, W.S., Matthews, G.J., Viola, V.E., Clark, R.G.: Phys. Rev. Lett. **35**, 988 (1975)
8. McClenahan, C.R., Segel, R.E.: Phys. Rev. C **11**, 370 (1975)
9. Poppe, C.H., Anderson, J.D., Davis, J.C., Grimes, S.M., Wong, C.: Phys. Rev. C **14**, 438 (1976)
10. Risler, R., Grüebler, W., Debenham, A.A., König, V., Schmelzbach, P.A., Boerma, D.O.: Nucl. Phys. A **286**, 115 (1977)
11. J. Ulbricht: private communication
12. Ulbricht, J., Arnold, W., Berg, H., Clausnitzer, G., Huttel, E., Krause, H.H.: Nucl. Phys. A **287**, 220 (1977)
13. Kurath, D.: Phys. Rev. **101**, 216 (1956)
14. Barker, F.C.: Nucl. Phys. **83**, 418 (1966)
15. Cohen, S., Kurath, D.: Nucl. Phys. **73**, 1 (1965); A **101**, 1 (1967); A **141**, 145 (1970)
16. Kumar, N.: Nucl. Phys. A **225**, 221 (1974)
17. Kumar, N., Barker, F.C.: Nucl. Phys. A **167**, 434 (1971)
18. Bouten, M., van Leuven, P., Depuydt, H., Schotsmans, L.: Nucl. Phys. A **100**, 90 (1967)
19. Elliott, J.P.: Proc. Roy. Soc. A **245**, 128 (1958); 562 (1958)
20. Arickx, F., van Leuven, P., Bouten, M.: Nucl. Phys. A **252**, 416 (1975)
21. Arickx, F.: Nucl. Phys. A **268**, 347 (1976)
22. Fick, D., Hackenbroich, H.H., Seligman, T.H., Zahn, W.: Phys. Lett. **62** B, 121 (1976)
23. Stöwe, H., Zahn, W.: Nucl. Phys. A **286**, 89 (1977)
24. Stöwe, H., Zahn, W.: Nucl. Phys. A **289**, 317 (1977)
25. Čaplar, R., Fick, D., Gemmeke, H., Hackenbroich, H.H., Lassen, L., Seligman, T.H., Zahn, W.: Verhandl. DPG (VI) **12**, 835 (1977)
26. Hackenbroich, H.H.: Symposium on Present Status and Novel Developments in the Nuclear Many-Body Problem, Rome, Bologna: Editrice Compositori 1973
27. Zahn, W.: J. Phys. G **3**, L209 (1977)
28. Stöwe, H., Zahn, W.: Verhandl. DPG (VI) **12**, 835 (1977)
29. Le-Chi-Niem, Heiss, P., Hackenbroich, H.H.: Z. Physik **244**, 346 (1971)
30. Plattner, R.: Resonances, Poles and Polarization, Lecture Notes in Physics, Vol. 30, p. 162, Berlin-Heidelberg-New York: Springer 1974
31. Hackenbroich, H.H., Seligman, T.H.: Phys. Lett. **41** B, 102 (1972)

H. Stöwe
W. Zahn
Institut für Theoretische Physik
der Universität zu Köln
Zülpicher Strasse 77
D-5000 Köln 41
Federal Republic of Germany